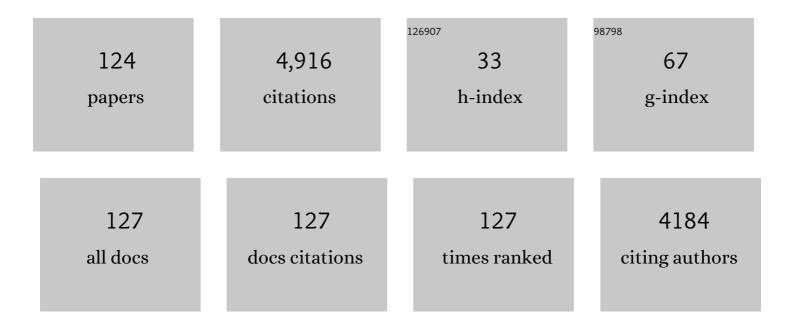
## Yoshiki Higuchi

List of Publications by Year in descending order

Source: https://exaly.com/author-pdf/1573650/publications.pdf Version: 2024-02-01



#	Article	IF	CITATIONS
1	Unusual ligand structure in Ni–Fe active center and an additional Mg site in hydrogenase revealed by high resolution X-ray structure analysis. Structure, 1997, 5, 1671-1680.	3.3	374
2	The DIX domain of Dishevelled confers Wnt signaling by dynamic polymerization. Nature Structural and Molecular Biology, 2007, 14, 484-492.	8.2	365
3	Removal of the bridging ligand atom at the Ni–Fe active site of [NiFe] hydrogenase upon reduction with H2, as revealed by X-ray structure analysis at 1.4 à resolution. Structure, 1999, 7, 549-556.	3.3	333
4	Structural basis for a [4Fe-3S] cluster in the oxygen-tolerant membrane-bound [NiFe]-hydrogenase. Nature, 2011, 479, 253-256.	27.8	262
5	Activation Process of [NiFe] Hydrogenase Elucidated by High-Resolution X-Ray Analyses: Conversion of the Ready to the Unready State. Structure, 2005, 13, 1635-1642.	3.3	248
6	Structural Studies of the Carbon Monoxide Complex of [NiFe]hydrogenase from Desulfovibrio vulgaris Miyazaki F:  Suggestion for the Initial Activation Site for Dihydrogen. Journal of the American Chemical Society, 2002, 124, 11628-11635.	13.7	235
7	Crystal structure of DMA photolyase from Anacystis nidulans. Nature Structural and Molecular Biology, 1997, 4, 887-891.	8.2	196
8	Single Crystal EPR Studies of the Reduced Active Site of [NiFe] Hydrogenase fromDesulfovibrio vulgarisMiyazaki F. Journal of the American Chemical Society, 2003, 125, 83-93.	13.7	196
9	[NiFe] hydrogenases: structural and spectroscopic studies of the reaction mechanism. Dalton Transactions, 2009, , 7577.	3.3	179
10	Cytochrome <i>c</i> polymerization by successive domain swapping at the C-terminal helix. Proceedings of the National Academy of Sciences of the United States of America, 2010, 107, 12854-12859.	7.1	148
11	A single-crystal ENDOR and density functional theory study of the oxidized states of the [NiFe] hydrogenase from Desulfovibrio vulgaris Miyazaki F. Journal of Biological Inorganic Chemistry, 2006, 11, 41-51.	2.6	103
12	Structure and function of [NiFe] hydrogenases. Journal of Biochemistry, 2016, 160, 251-258.	1.7	92
13	Crystal Structures of Ethanolamine Ammonia-lyase Complexed with Coenzyme B12 Analogs and Substrates. Journal of Biological Chemistry, 2010, 285, 26484-26493.	3.4	87
14	"Newton's cradle―proton relay with amide–imidic acid tautomerization in inverting cellulase visualized by neutron crystallography. Science Advances, 2015, 1, e1500263.	10.3	80
15	Dual gas-diffusion membrane- and mediatorless dihydrogen/air-breathing biofuel cell operating at room temperature. Journal of Power Sources, 2016, 335, 105-112.	7.8	67
16	Structural Study Reveals That Ser-354 Determines Substrate Specificity on Human Histidine Decarboxylase. Journal of Biological Chemistry, 2012, 287, 29175-29183.	3.4	65
17	Direct electron transfer-type dual gas diffusion H <sub>2</sub> /O <sub>2</sub> biofuel cells. Journal of Materials Chemistry A, 2016, 4, 8742-8749.	10.3	61
18	Nylon-oligomer Degrading Enzyme/Substrate Complex: Catalytic Mechanism of 6-Aminohexanoate-dimer Hydrolase. Journal of Molecular Biology, 2007, 370, 142-156.	4.2	53

#	Article	IF	CITATIONS
19	Xâ€ray structure of a twoâ€domain type laccase: A missing link in the evolution of multiâ€copper proteins. FEBS Letters, 2009, 583, 1189-1195.	2.8	53
20	Structural insights into the O <sub>2</sub> reduction mechanism of multicopper oxidase. Journal of Biochemistry, 2015, 158, 293-298.	1.7	53
21	Single crystal EPR study of the Ni center of NiFe hydrogenase. Chemical Physics Letters, 1996, 256, 518-524.	2.6	48
22	Three-dimensional Structure of Nylon Hydrolase and Mechanism of Nylon-6 Hydrolysis. Journal of Biological Chemistry, 2012, 287, 5079-5090.	3.4	48
23	Structural and oxygen binding properties of dimeric horse myoglobin. Dalton Transactions, 2012, 41, 11378.	3.3	47
24	Structural basis of the redox switches in the NAD <sup>+</sup> -reducing soluble [NiFe]-hydrogenase. Science, 2017, 357, 928-932.	12.6	46
25	Single crystals of hydrogenase from Desulfovibrio vulgaris Miyazaki F. Journal of Biological Chemistry, 1987, 262, 2823-5.	3.4	44
26	Studies on hydrogenase. Proceedings of the Japan Academy Series B: Physical and Biological Sciences, 2013, 89, 16-33.	3.8	43
27	Structural basis for cargo binding and autoinhibition of Bicaudal-D1 by a parallel coiled-coil with homotypic registry. Biochemical and Biophysical Research Communications, 2015, 460, 451-456.	2.1	43
28	Domain Swapping of the Heme and N-Terminal α-Helix in <i>Hydrogenobacter thermophilus</i> Cytochrome <i>c</i> <sub>552</sub> Dimer. Biochemistry, 2012, 51, 8608-8616.	2.5	41
29	Control of the Transition between Ni  and Niâ€SI <sub>a</sub> States by the Redox State of the Proximal FeS Cluster in the Catalytic Cycle of [NiFe] Hydrogenase. Angewandte Chemie - International Edition, 2014, 53, 13817-13820.	13.8	41
30	Structural Basis for the Reaction Mechanism of S-Carbamoylation of HypE by HypF in the Maturation of [NiFe]-Hydrogenases. Journal of Biological Chemistry, 2012, 287, 28409-28419.	3.4	40
31	Formation of Oligomeric Cytochrome <i>c</i> during Folding by Intermolecular Hydrophobic Interaction between N- and C-Terminal α-Helices. Biochemistry, 2013, 52, 8732-8744.	2.5	40
32	X-ray Crystallographic Analysis of the 6-Aminohexanoate Cyclic Dimer Hydrolase. Journal of Biological Chemistry, 2010, 285, 1239-1248.	3.4	38
33	Domain-swapped cytochrome cb <sub>562</sub> dimer and its nanocage encapsulating a Zn–SO <sub>4</sub> cluster in the internal cavity. Chemical Science, 2015, 6, 7336-7342.	7.4	37
34	Crystal Structure of CO-sensing Transcription Activator CooA Bound to Exogenous Ligand Imidazole. Journal of Molecular Biology, 2007, 367, 864-871.	4.2	35
35	Comprehensive reaction mechanisms at and near the Ni–Fe active sites of [NiFe] hydrogenases. Dalton Transactions, 2018, 47, 4408-4423.	3.3	34
36	The presence of a SO molecule in [NiFe] hydrogenase from Desulfovibrio vulgaris Miyazaki as detected by mass spectrometry. Journal of Inorganic Biochemistry, 2000, 80, 205-211.	3.5	33

#	Article	IF	CITATIONS
37	Positively charged residues located downstream of PIP box, together with TD amino acids within PIP box, are important for CRL4Cdt2-mediated proteolysis. Genes To Cells, 2011, 16, 12-22.	1.2	33
38	The PHCCEx domain of Tiam1/2 is a novel protein- and membrane-binding module. EMBO Journal, 2010, 29, 236-250.	7.8	31
39	Rational Design of Heterodimeric Protein using Domain Swapping for Myoglobin. Angewandte Chemie - International Edition, 2015, 54, 511-515.	13.8	31
40	Cysteine SH and Glutamate COOH Contributions to [NiFe] Hydrogenase Proton Transfer Revealed by Highly Sensitive FTIR Spectroscopy. Angewandte Chemie - International Edition, 2019, 58, 13285-13290.	13.8	31
41	Crystal Structures of Hydrogenase Maturation Protein HypE in the Apo and ATP-bound Forms. Journal of Molecular Biology, 2007, 372, 1045-1054.	4.2	30
42	Crystal structure analysis of the translation factor RF3 (release factor 3). FEBS Letters, 2012, 586, 3705-3709.	2.8	30
43	Structural and enzymatic characterization of BacD, an <scp>L</scp> â€amino acid dipeptide ligase from <i>Bacillus subtilis</i> . Protein Science, 2012, 21, 707-716.	7.6	30
44	Refined Regio- and Stereoselective Hydroxylation of <scp>l</scp> -Pipecolic Acid by Protein Engineering of <scp>l</scp> -Proline <i>cis</i> -4-Hydroxylase Based on the X-ray Crystal Structure. ACS Synthetic Biology, 2015, 4, 383-392.	3.8	30
45	FT-IR Characterization of the Light-Induced Ni-L2 and Ni-L3 States of [NiFe] Hydrogenase from <i>Desulfovibrio vulgaris</i> Miyazaki F. Journal of Physical Chemistry B, 2015, 119, 13668-13674.	2.6	28
46	An Oâ€Centered Structure of the Trinuclear Copper Center in the Cys500Ser/Glu506Gln Mutant of CueO and Structural Changes in Low to High Xâ€Ray Dose Conditions. Angewandte Chemie - International Edition, 2012, 51, 1861-1864.	13.8	26
47	Crystal structure analysis of <i>Bacillus subtilis</i> ferredoxinâ€NADP <sup>+</sup> oxidoreductase and the structural basis for its substrate selectivity. Protein Science, 2010, 19, 2279-2290.	7.6	25
48	Formation of Domain-Swapped Oligomer of Cytochrome <i>c</i> from Its Molten Globule State Oligomer. Biochemistry, 2014, 53, 4696-4703.	2.5	24
49	Inhibitory activity of Filipendula ulmaria constituents on recombinant human histidine decarboxylase. Food Chemistry, 2013, 138, 1551-1556.	8.2	23
50	New insights into the catalytic active-site structure of multicopper oxidases. Acta Crystallographica Section D: Biological Crystallography, 2014, 70, 772-779.	2.5	23
51	Light-Driven Hydrogen Production by Hydrogenases and a Ru-Complex inside a Nanoporous Glass Plate under Aerobic External Conditions. Journal of Physical Chemistry Letters, 2014, 5, 2402-2407.	4.6	23
52	Reactivation of standard [NiFe]-hydrogenase and bioelectrochemical catalysis of proton reduction and hydrogen oxidation in a mediated-electron-transfer system. Bioelectrochemistry, 2018, 123, 156-161.	4.6	22
53	Two alternative modes for optimizing nylonâ€6 byproduct hydrolytic activity from a carboxylesterase with a l²â€lactamase fold: Xâ€ray crystallographic analysis of directly evolved 6â€aminohexanoateâ€dimer hydrolase. Protein Science, 2009, 18, 1662-1673.	7.6	21
54	Direct Participation of a Peripheral Side Chain of a Corrin Ring in Coenzymeâ€B <sub>12</sub> Catalysis. Angewandte Chemie - International Edition, 2018, 57, 7830-7835.	13.8	20

#	Article	IF	CITATIONS
55	Domain-Swapped Dimer of Pseudomonas aeruginosa Cytochrome c551: Structural Insights into Domain Swapping of Cytochrome c Family Proteins. PLoS ONE, 2015, 10, e0123653.	2.5	19
56	Change in structure and ligand binding properties of hyperstable cytochrome <i>c</i> <sub>555</sub> from <scp><i>A</i></scp> <i>quifex aeolicus</i> by domain swapping. Protein Science, 2015, 24, 366-375.	7.6	18
57	Gas-diffusion and Direct-electron-transfer-type Bioanode for Hydrogen Oxidation with Oxygen-tolerant [NiFe]-hydrogenase as an Electrocatalyst. Chemistry Letters, 2014, 43, 1575-1577.	1.3	17
58	Bioelectrochemical analysis of thermodynamics of the catalytic cycle and kinetics of the oxidative inactivation of oxygen-tolerant [NiFe]-hydrogenase. Journal of Electroanalytical Chemistry, 2016, 766, 152-161.	3.8	17
59	Concerto catalysis—harmonising [NiFe]hydrogenase and NiRu model catalysts. Dalton Transactions, 2010, 39, 2993.	3.3	16
60	Kinetic Analysis of Inactivation and Enzyme Reaction of Oxygen-Tolerant [NiFe]-Hydrogenase at Direct Electron-Transfer Bioanode. Bulletin of the Chemical Society of Japan, 2014, 87, 1177-1185.	3.2	16
61	Photoactivation of the Ni-SI <sub>r</sub> state to the Ni-SI <sub>a</sub> state in [NiFe] hydrogenase: FT-IR study on the light reactivity of the ready Ni-SI <sub>r</sub> state and as-isolated enzyme revisited. Physical Chemistry Chemical Physics, 2016, 18, 22025-22030.	2.8	16
62	Structure and molecular evolution of multicopper blue proteins. Biomolecular Concepts, 2010, 1, 31-40.	2.2	15
63	How Coenzyme B <sub>12</sub> -Dependent Ethanolamine Ammonia-Lyase Deals with Both Enantiomers of 2-Amino-1-propanol as Substrates: Structure-Based Rationalization,,. Biochemistry, 2011, 50, 591-598.	2.5	15
64	Oligomerization enhancement and two domain swapping mode detection for thermostable cytochrome c <sub>552</sub> via the elongation of the major hinge loop. Molecular BioSystems, 2015, 11, 3218-3221.	2.9	15
65	A direct heterotypic interaction between the DIX domains of Dishevelled and Axin mediates signaling to β-catenin. Science Signaling, 2019, 12, .	3.6	15
66	Crystallization and preliminary X-ray crystallographic studies of the axin DIX domain. Acta Crystallographica Section F: Structural Biology Communications, 2007, 63, 529-531.	0.7	14
67	Phase-diagram-guided method for growth of a large crystal of glycoside hydrolase family 45 inverting cellulase suitable for neutron structural analysis. Journal of Synchrotron Radiation, 2013, 20, 859-863.	2.4	14
68	Redox-dependent conformational changes of a proximal [4Fe–4S] cluster in Hyb-type [NiFe]-hydrogenase to protect the active site from O <sub>2</sub> . Chemical Communications, 2018, 54, 12385-12388.	4.1	14
69	Redox Potentialâ€Đependent Formation of an Unusual His–Trp Bond in Bilirubin Oxidase. Chemistry - A European Journal, 2018, 24, 18052-18058.	3.3	14
70	Domain swapping oligomerization of thermostable c-type cytochrome in E. coli cells. Scientific Reports, 2016, 6, 19334.	3.3	13
71	Formation and carbon monoxideâ€dependent dissociation of <i>Allochromatium vinosum</i> cytochrome <i>c</i> ′ oligomers using domainâ€swapped dimers. Protein Science, 2017, 26, 464-474.	7.6	13
72	Molecular dynamics studies on the mutational structures of a nylon-6 byproduct-degrading enzyme. Chemical Physics Letters, 2011, 507, 157-161.	2.6	12

#	Article	IF	CITATIONS
73	Structural aspects of [NiFe]-hydrogenases. Reviews in Inorganic Chemistry, 2013, 33, 173-192.	4.1	11
74	Photosensitivity of the Ni-A state of [NiFe] hydrogenase from Desulfovibrio vulgaris Miyazaki F with visible light. Biochemical and Biophysical Research Communications, 2013, 430, 284-288.	2.1	11
75	Equilibrium between inactive ready Ni-SI <sub>r</sub> and active Ni-SI <sub>a</sub> states of [NiFe] hydrogenase studied by utilizing Ni-SI <sub>r</sub> -to-Ni-SI <sub>a</sub> photoactivation. Chemical Communications, 2017, 53, 10444-10447.	4.1	11
76	Rational Design of Domainâ€5wappingâ€Based <i>c</i> â€Type Cytochrome Heterodimers by Using Chimeric Proteins. ChemBioChem, 2017, 18, 1712-1715.	2.6	11
77	Cysteine SH and Glutamate COOH Contributions to [NiFe] Hydrogenase Proton Transfer Revealed by Highly Sensitive FTIR Spectroscopy. Angewandte Chemie, 2019, 131, 13419-13424.	2.0	11
78	Structural Basis of the Function of [NiFe]-hydrogenases. Chemistry Letters, 2020, 49, 164-173.	1.3	11
79	Crystal structure of the CueO mutants at Glu506, the key amino acid located in the proton transfer pathway for dioxygen reduction. Biochemical and Biophysical Research Communications, 2013, 438, 686-690.	2.1	10
80	Purification, crystallization and preliminary X-ray analysis of human histidine decarboxylase. Acta Crystallographica Section F: Structural Biology Communications, 2012, 68, 675-677.	0.7	9
81	Catalytic cycle of cytochrome- c 3 hydrogenase, a [NiFe]-enzyme, deduced from the structures of the enzyme mimic. International Journal of Hydrogen Energy, 2014, 39, 18543-18550.	7.1	9
82	Electrostatic roles in electron transfer from [NiFe] hydrogenase to cytochrome c 3 from Desulfovibrio vulgaris Miyazaki F. Biochimica Et Biophysica Acta - Proteins and Proteomics, 2017, 1865, 481-487.	2.3	8
83	Construction of a Triangleâ€Shaped Trimer and a Tetrahedron Using an αâ€Helixâ€Inserted Circular Permutant of Cytochrome <i>c</i> <sub>555</sub> . Chemistry - an Asian Journal, 2018, 13, 964-967.	3.3	8
84	Complete Genome Sequence of a Moderately Thermophilic Facultative Chemolithoautotrophic Hydrogen-Oxidizing Bacterium, Hydrogenophilus thermoluteolus TH-1. Microbiology Resource Announcements, 2018, 7, .	0.6	8
85	A functional role of the glycosylated N-terminal domain of chondromodulin-I. Journal of Bone and Mineral Metabolism, 2011, 29, 23-30.	2.7	7
86	Structural basis of the correct subunit assembly, aggregation, and intracellular degradation of nylon hydrolase. Scientific Reports, 2018, 8, 9725.	3.3	7
87	Protein surface charge effect on 3D domain swapping in cells for c-type cytochromes. Biochimica Et Biophysica Acta - Proteins and Proteomics, 2019, 1867, 140265.	2.3	7
88	Crystal structure of NADH:rubredoxin oxidoreductase from <i>Clostridium acetobutylicum</i> : A key component of the dioxygen scavenging system in obligatory anaerobes. Proteins: Structure, Function and Bioinformatics, 2010, 78, 1066-1070.	2.6	6
89	Improved purification, crystallization and crystallographic study of Hyd-2-type [NiFe]-hydrogenase from <i>Citrobacter</i> sp. S-77. Acta Crystallographica Section F, Structural Biology Communications, 2016, 72, 53-58.	0.8	6
90	Structural basis for Ccd1 auto-inhibition in the Wnt pathway through homomerization of the DIX domain. Scientific Reports, 2017, 7, 7739.	3.3	6

#	Article	IF	CITATIONS
91	High-resolution structure of a Y27W mutant of the Dishevelled2 DIX domain. Acta Crystallographica Section F, Structural Biology Communications, 2019, 75, 116-122.	0.8	6
92	Crystallization and preliminary X-ray diffraction analysis of membrane-bound respiratory [NiFe] hydrogenase from <i>Hydrogenovibrio marinus</i> . Acta Crystallographica Section F: Structural Biology Communications, 2011, 67, 827-829.	0.7	5
93	Synthesis and Reactivity of a Water-soluble NiRu Monohydride Complex with a Tethered Pyridine Moiety. Chemistry Letters, 2016, 45, 197-199.	1.3	5
94	New assay method based on Raman spectroscopy for enzymes reacting with gaseous substrates. Protein Science, 2019, 28, 663-670.	7.6	5
95	3D domain swapping of azurin from <i>Alcaligenes xylosoxidans</i> . Metallomics, 2020, 12, 337-345.	2.4	5
96	Thermodynamic Control of Domain Swapping by Modulating the Helical Propensity in the Hinge Region of Myoglobin. Chemistry - an Asian Journal, 2020, 15, 1743-1749.	3.3	5
97	Role of π-Electron Systems in Stabilization of the Oxidized Tetraheme Architecture in Cytochrome <i>c</i> 3. Bulletin of the Chemical Society of Japan, 2011, 84, 1096-1101.	3.2	4
98	Crystallographic characterization of the C-terminal coiled-coil region of mouse Bicaudal-D1 (BICD1). Acta Crystallographica Section F, Structural Biology Communications, 2014, 70, 1103-1106.	0.8	4
99	Exogenous acetate ion reaches the type II copper centre in CueO through the water-excretion channel and potentially affects the enzymatic activity. Acta Crystallographica Section F, Structural Biology Communications, 2016, 72, 558-563.	0.8	4
100	Crystal structure of a hypothetical protein, TTHA0829 from Thermus thermophilus HB8, composed of cystathionine-β-synthase (CBS) and aspartate-kinase chorismate-mutase tyrA (ACT) domains. Extremophiles, 2016, 20, 275-282.	2.3	4
101	Rational design of metal-binding sites in domain-swapped myoglobin dimers. Journal of Inorganic Biochemistry, 2021, 217, 111374.	3.5	4
102	Enzymatic synthesis of nylon-6 units in organic solvents containing low concentrations of water. Journal of Molecular Catalysis B: Enzymatic, 2010, 64, 81-88.	1.8	3
103	Crystallization and preliminary X-ray studies of ferredoxin-NADP <sup>+</sup> oxidoreductase encoded by <i>Bacillus subtilis</i> yumC. Acta Crystallographica Section F: Structural Biology Communications, 2010, 66, 301-303.	0.7	3
104	Crystallization and X-ray diffraction analysis of nylon-oligomer hydrolase (NylC) fromAgromycessp. KY5R. Acta Crystallographica Section F: Structural Biology Communications, 2011, 67, 892-895.	0.7	3
105	Crystallization and X-ray diffraction analysis of nylon hydrolase (NylC) fromArthrobactersp. KI72. Acta Crystallographica Section F: Structural Biology Communications, 2013, 69, 1151-1154.	0.7	3
106	Crystallization and preliminary X-ray analysis of the NAD <sup>+</sup> -reducing [NiFe] hydrogenase from <i>Hydrogenophilus thermoluteolus</i> TH-1. Acta Crystallographica Section F, Structural Biology Communications, 2015, 71, 96-99.	0.8	3
107	Ni-elimination from the active site of the standard [NiFe]â€ <sup>4</sup> hydrogenase upon oxidation by O2. Journal of Inorganic Biochemistry, 2017, 177, 435-437.	3.5	3
108	Structural Changes of the Trinuclear Copper Center in Bilirubin Oxidase upon Reduction. Molecules, 2019, 24, 76.	3.8	3

#	Article	IF	CITATIONS
109	Crystallization and preliminary X-ray analysis of NADH:rubredoxin oxidoreductase from <i>Clostridium acetobutylicum</i> . Acta Crystallographica Section F: Structural Biology Communications, 2010, 66, 23-25.	0.7	2
110	Nanoscale charge transport in cytochromec3/DNA network: Comparative studies between redox-active molecules. Japanese Journal of Applied Physics, 2015, 54, 095201.	1.5	2
111	Biochemical, spectroscopic and X-ray structural analysis of deuterated multicopper oxidase CueO prepared from a new expression construct for neutron crystallography. Acta Crystallographica Section F, Structural Biology Communications, 2016, 72, 788-794.	0.8	2
112	Towards cryogenic neutron crystallography on the reduced form of [NiFe]-hydrogenase. Acta Crystallographica Section D: Structural Biology, 2020, 76, 946-953.	2.3	2
113	Experimental and theoretical study on converting myoglobin into a stable domain-swapped dimer by utilizing a tight hydrogen bond network at the hinge region. RSC Advances, 2021, 11, 37604-37611.	3.6	2
114	Crystallization and preliminary X-ray analysis of a class II release factor RF3 from a sulfate-reducing bacterium. Acta Crystallographica Section F: Structural Biology Communications, 2008, 64, 622-624.	0.7	1
115	Expression, crystallization and preliminary X-ray crystallographic study of ethanolamine ammonia-lyase from <i>Escherichia coli</i> . Acta Crystallographica Section F: Structural Biology Communications, 2010, 66, 709-711.	0.7	1
116	Crystallographic characterization of the DIX domain of the Wnt signalling positive regulator Ccd1. Acta Crystallographica Section F: Structural Biology Communications, 2011, 67, 758-761.	0.7	1
117	Crystallographic analysis of FAD-dependent glucose dehydrogenase. Acta Crystallographica Section F, Structural Biology Communications, 2015, 71, 1017-1019.	0.8	1
118	Mutations affecting the internal equilibrium of the reaction catalyzed by 6â€aminohexanoateâ€dimer hydrolase. FEBS Letters, 2016, 590, 3133-3143.	2.8	1
119	The Challenge of Visualizing the Bridging Hydride at the Active Site and Proton Network of [NiFe]-Hydrogenase by Neutron Crystallography. Topics in Catalysis, 2021, 64, 622-630.	2.8	1
120	Purification, crystallization and preliminary X-ray analysis of the dissimilatory sulfite reductase fromDesulfovibrio vulgarisMiyazaki F. Acta Crystallographica Section F: Structural Biology Communications, 2010, 66, 1470-1472.	0.7	0
121	Crystallization and preliminary X-ray analysis of dimeric and trimeric cytochromescfrom horse heart. Acta Crystallographica Section F: Structural Biology Communications, 2010, 66, 1477-1479.	0.7	0
122	Structure and Function of [NiFe] Hydrogenase Seibutsu Butsuri, 2000, 40, 249-253.	0.1	0
123	Head-to-Tail Complex of Dishevelled and Axin-DIX Domains: Expression, Purification, Crystallographic Studies and Packing Analysis. Protein and Peptide Letters, 2019, 26, 792-797.	0.9	0
124	Structural and spectroscopic characterization of CO inhibition of [NiFe]-hydrogenase from <i>Citrobacter</i> sp. S-77. Acta Crystallographica Section F, Structural Biology Communications, 2022, 78, 66-74.	0.8	0